AIAA JOURNAL
Vol. 35, No. 10, October 1997

# Mean and Turbulence Measurements in the Near Field of a Wingtip Vortex

Jim S. Chow*
*Institute for Defense Analyses, Alexandria, Virginia 22311*
Gregory G. Zilliac†
*NASA Ames Research Center, Moffett Field, California 94035*
and
Peter Bradshaw‡
*Stanford University, Stanford, California 94305*

**The rollup of a wingtip vortex, at a Reynolds number based on chord of $4.6 \times 10^6$, was studied with an emphasis on suction side and very near-wake measurements (up to $x/c = 0.678$ downstream of the trailing edge). The research was conducted in a $32 \times 48$ in. ($0.81 \times 1.22$ m), low-speed wind tunnel. The rectangular half-wing model had a semispan of 36 in. (0.91 m), a chord of 48 in. (1.22 m), and a rounded tip. Seven-hole pressure probe measurements of the velocity field surrounding the wingtip showed that a large axial velocity up to $1.77U_\infty$ developed in the vortex core. This high a level of core axial velocity has not been measured previously. Triple-wire probes were used to measure all components of the Reynolds stress tensor. It was determined from correlation measurements that meandering of the vortex was small and did not contribute appreciably to turbulence measurements. The flow was found to be turbulent in the near field (as high as 24% rms velocity), and the turbulence decayed quickly with streamwise distance because of the stabilizing effect of the nearly solid body rotation of the vortex-core mean flow. A streamwise variation of the location of peak levels of turbulence, relative to the core centerline, was also noted. Close to the trailing edge of the wing, peak shear stress levels were measured at the edge of the vortex core, whereas in the most downstream wake plane, the peak levels were measured at a radius roughly equal to one-third of the vortex core radius. The Reynolds shear stresses (in Cartesian coordinates) were not aligned with the mean strain rate, indicating that an isotropic-eddy-viscosity-based prediction method cannot fully model the turbulence in the vortex. In cylindrical coordinates, with the origin at the vortex centerline, the radial normal stress was found to be larger than the circumferential component.**



## Introduction

THE wingtip vortex flow is of great importance because of its effect on practical problems such as landing separation distances for aircraft, blade/vortex interactions on helicopter blades, and propeller cavitation on ships. It also continues to be a perplexing problem for computational scientists because of the presence of large gradients of velocity and pressure in all three dimensions, especially in the near field at high Reynolds number.

In the case of a wing with nearly elliptic loading, a discrete vortex forms at the tip (Fig. 1), fed by vorticity from the boundary layer near the tip. As the vortex moves downstream, it rolls up more and more of the wing wake until its circulation is nominally equal to that of the wing. The rollup distance is small compared with the separation of aircraft on the approach path but not necessarily small compared with the distance between interacting lifting surfaces, such as the strake or foreplane and the main wing on a close-coupled fighter or consecutive blades on a helicopter rotor. The flow in the near-field rollup region is therefore important in its own right as well as providing a possible means of control of the far-field vortex.

Review of the literature indicates that the tip vortex has been the subject of hundreds of studies. The emphasis of most of these studies has been on mean velocity measurements in the far field. Few Navier–Stokes computational studies and even fewer experimental investigations of the near-field vortex rollup process exist.

Received Aug. 16, 1996; revision received May 27, 1997; accepted for publication June 20, 1997. 

*Research Staff Member.
†Research Scientist, Fluid Mechanics Laboratory.
‡Professor, Mechanical Engineering Department. Member AIAA.

The computational studies by Dacles-Marianiet al.,[1] done in conjunction with this experimental study, have shown that it is possible to predict the mean flow of the tip-vortex near field rather well by using a Reynolds-averaged Navier–Stokes code; however, the turbulence modeling used was not as accurate as desired.

The eddy viscosity analysis of Hoffmann and Joubert[2] is one of few analytic studies of the turbulent trailing vortex. They predicted a logarithmic radial variation of circulation near the edge of the vortex core. Batchelor[3] and Moore and Saffman[4] have investigated fully rolled-up laminar trailing vortices. However, at the Reynolds numbers found in most practical applications, trailing vortices are nominally turbulent. Squire[5] attempted to model a turbulent vortex by using a constant eddy viscosity and had limited success.

There have been several experimental studies of the fully developed vortex far downstream of the wingtip, including parametric studies where various tip shapes[6] and devices were used to alter or manipulate the tip vortex.[7] These studies, which were related to helicopter blades rather than fixed wings, concluded that tip shape can substantially affect the way the vorticity in the tip vortex is concentrated. However, tradeoffs with drag make more experimental work necessary before reliable tip modifications can be made.

Other experimental work on the flow over the tip and in the rollup region, e.g., Ref. 8 and related work of Chigier and Corsiglia,[9] showed a characteristic surface-pressure suction peak near the tip, denoting the approximate location of the tip vortex as it develops on the top surface of the wing. Other features noted by Chigier (for the square-tipped wing) were a relatively high axial velocity in the core of the vortex in the near field ($u/U_\infty = 1.1$ to 1.4 at $\alpha = 12$ deg, where $u$ is the $x$ component of velocity and $\alpha$ is the angle of attack) and a secondary vortex with the same sense of rotation as the main vortex, located between the main vortex and the wingtip.

Green[10] obtained measurements with double-pulsed holography on a rectangular planform wing with rounded tip at a Reynolds number based on chord of about $7 \times 10^5$. When these measurements were

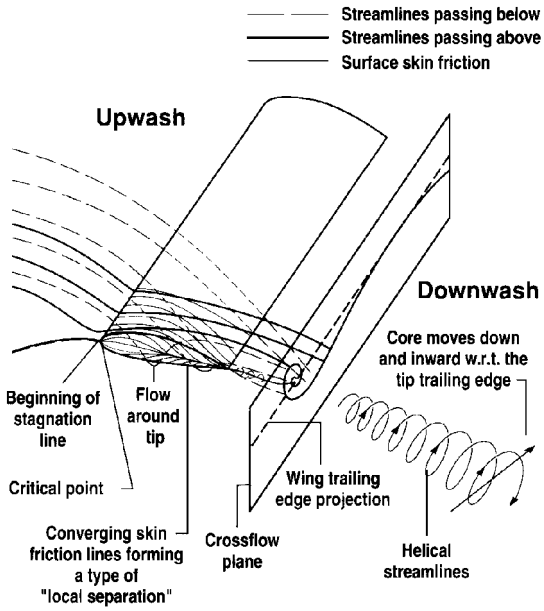


**Fig. 1 Initial rollup of a wingtip vortex.**

used in conjunction with the tailored-air-bubble technique, the instantaneous flow velocity and core static pressure were determined. At a 10-deg angle of attack, the averaged (based on a limited number of occurrences) axial velocity in the core of the vortex was 1.6 times the freestream velocity and the mean pressure drop from the freestream to the core was about 3.3 times the freestream dynamic pressure.

Mehta and Cantwell[11] measured two of the three Reynolds shear stresses in a turbulent vortex generated by a half-delta wing at relatively low Reynolds number. Distributions of Reynolds shear stresses were found to be consistent with the eddy viscosity concept, and the distributions of $\overline{vw}$ ($\overline{uw}$, $\overline{vw}$, and $\overline{ww}$ are the Reynolds normal stresses) aligned so that their contribution to vorticity production was negligible.

Bandyopadhyay et al.[12] investigated the turbulence structure in a turbulent trailing vortex and concluded that, for their range of test conditions, the Rossby number (axial velocity defect/maximum tangential velocity) was the controlling parameter for the turbulence structure and not the vortex Reynolds number (circulation/viscosity). They also concluded that the inner core is not, as suggested previously, a region of solid-body rotation that does not interact with the outer vortex region but rather is a relaminarizing region where patches of turbulent fluid are intermittently brought in from the outer region. However, their vortex was created by a double-wing vortex generator, and their measurements, taken far downstream of the trailing edge, may not be quantitatively representative of the near-field rollup region of a wingtip vortex.

The issue of vortex meander and its influence on measurements in the vortex region is a major concern with many experimental studies of vortices. The crux of the meander problem is that low-frequency motion of a vortex can be misinterpreted as true turbulence. Westphal and Mehta[13] made turbulence measurements downstream of an oscillating vortex and compared them with results for a stationary vortex. They found that $\hat{v}$ (where $\hat{u}$, $\hat{v}$, $\hat{w}$ are the $x$, $y$, $z$ components of rms velocity) increased by a factor of 2 and that contours of the Reynolds shear stresses were altered considerably for a meandering vortex.

McAlister and Takahashi[14] used laser Doppler velocimetry to measure the mean velocity field of a meandering trailing vortex. They observed a slow periodic spanwise oscillation of the vortex ($fc/U_\infty$ on the order of 0.01, where $f$ is the oscillation frequency and $c$ is the wing chord) and used conditional sampling methods to extract the "true" flowfield. Devenport et al.[15] obtained turbulence and mean field measurements from $x/c = 5.0$ to 30.0 behind a rectangular NACA 0012 wing by using seven-hole and four-wire probes. High turbulent stress measured in the core region was attributed primarily to meandering of their vortex. They found the meandering amplitudes increased approximately linearly with downstream distance and decreased with angle of attack. Some additional insight into the turbulent structure of the vortex cores was obtained through the use of high-pass filtering of the measurements.

There seems to have been no study of the tip flow and near-field vortex rollup process detailed enough to be used in developing or testing a prediction method or for putting the design of tip modifications on a firm fundamental basis. This experimental study focuses on the initial rollup region of the turbulent vortex from a generic wingtip at high Reynolds number. The approach is to first reach a basic understanding of the physics involved in the flow near the wingtip, supported by detailed measurements of turbulence structure, and then proceed to development of prediction methods or tip modifications, although both are in our program.

From the results acquired to date, we have been able to construct a detailed qualitative and quantitative picture of the process by which the tip boundary layer separates and rolls up into a vortex.

## Experimental Apparatus and Techniques

In our experiment, velocity-field measurements (by seven-hole pressure probe), single-wire correlation measurements, and turbulence measurements (by triple-wire probe) were obtained for the flow over a rectangular wing with rounded tip and up to 0.68 chord downstream of the trailing edge. The Reynolds number based on chord was $4.6 \times 10^6$.

The measurements were performed in the $32 \times 48$ in. ($0.81 \times 1.22$ m), low-speed wind tunnel located in the Fluid Mechanics Laboratory (FML) of NASA Ames Research Center. The maximum freestream turbulence level in the wind tunnel, measured by hot-wire anemometry, is 0.15%. A half-wing model of 4 ft (1.22 m) chord, 3 ft (0.91 m) semispan, rounded (body of revolution) wingtip, and NACA 0012 wing section was used, as shown in Fig. 2. The Cartesian coordinate system used to describe the physical locations of the experiment is also shown in Fig. 2. The origin is located at the root/trailing edge of the wing.

During the design phase of this study, the decision was made to use as large a model as possible while avoiding severe viscous tunnel interference because of excessive growth or separation of the tunnel-wall boundary layers. Inviscid tunnel interference is, of course, very large, and computations of this flowfield should take into account the presence of the tunnel walls (as has been done).[1]

The model was constructed of aluminum with a skin thickness of $\frac{1}{4}$ in. (6.4 mm) and precision machining of the surface contour ($\pm 0.0005$ in. or 0.01 mm). The angle of attack could be varied through $\pm 16$ deg by rotating the model about its quarter chord, although, as stated earlier, the only test case investigated in this study was at a $+10$-deg angle of attack. The quarter chord point was located in the vertical center of the test section.

A trip was used to fix transition near the leading edge. Roughness elements of 0.017-in. (0.43-mm) diameter were packed closely together to form a strip $\frac{1}{8}$ in. (3.2 mm) wide across the span of the wing at a surface distance of 2.0 in. (5.1 cm) from the leading edge. The trip extended around the tip and along the bottom surface

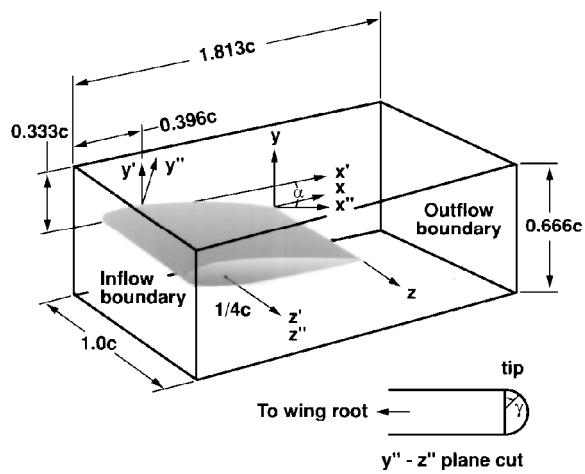


**Fig. 2 Wing model in test section with coordinate systems indicated.**

of the wing. Naphthalene sublimation, oil flows, and microphone techniques were used to confirm that the boundary layers on the suction side were turbulent and attached downstream of the trip.

Probe traversing was accomplished with custom-built rails and slides driven by Compumotor microstepping motors and controllers (25,000 microsteps/revolution). The five-degree-of-freedom traversing system had the capability of translation in three directions and of pitching and yawing the probe. Probe position and orientation were derived from optical encoders on all axes. Absolute positioning accuracy of a probe (relative to wing model surface) was within 0.02 in. Incremental positioning accuracy was determined to be within 0.001 in. (0.025 mm) for translation, 0.2 deg for pitch, and 0.1 deg for yaw.

A seven-hole pressure probe was used to measure static pressure and the velocity vector. The probe was calibrated in situ before installation of the model. The calibration procedure is described by Zilliac.[16] The data rate of the probe measurement system was maximized by use of simultaneous sampling of the eight required pressure measurements at each measurement location (seven for the probe and one for tunnel reference total) with eight separate MKS 223B pressure transducers. For high-flow angles (>30 deg), flow-angle measurement uncertainty for the seven-hole probe is within 1 deg, and velocity magnitude uncertainty is within 1.1% of the freestream velocity. For low-flow angles (<30 deg), flow-angle uncertainty is within 0.5 deg, and velocity magnitude uncertainty is within 0.8%.

Flowfield data using the seven-hole probe were taken at crossflow planes located at $x/c = \pm 1.14, \pm 0.591, \pm 0.394, \pm 0.296, \pm 0.197, \pm 0.114, \pm 0.005, 0.005, 0.125, 0.246, 0.452$, and 0.678. Data planes taken in the wake and upstream of the wing model had $21 \times 29$ data points (23.0 in. vertical or 0.58 m, and 28.0-in. or 0.71-m span). The boundaries of the data planes were at $z/c = 0.228$, $z/c = 0.825$, $y/c = \pm 0.11$, and $y/c = 0.47$. Data planes taken above the surface of the wing also had $21 \times 29$ data points. These planes, however, were half-planes because they extended exactly halfway around the tip but did not include any points below that line. For data points near the wing surface, an electronic touch sensor was used to find the surface of the model. The first vertical data point above the surface was taken 0.050 in. above the location found by the touch sensor. The grids were stretched so that the densest experimental grid spacing was around the center of the core of the vortex. The center of the core was found by taking a small grid (usually 15–20 points) of preliminary measurement data points around an estimated location of the core and then interpolating to the point with the lowest crossflow velocity.

A Dantec 55P91 triple-wire probe was used to measure turbulence quantities including triple products and all components of the Reynolds stress tensor. The probe consists of three nominally orthogonal 5-$\mu$m-diam, 0.05-in. (1.25 mm)-long, platinum-plated tungsten wires, which all lie within a 0.12-in. (3 mm) sphere. The exact orientation of the wires was determined by calibration. The outputs of the three wires were connected to custom-built NASA FML hot-wire bridges. Calibration was performed according to the method of LeBoeuf.[17] This method avoids the necessity of measuring the orientation of individual wires. Separate constant-angle and varying-angle calibrations were conducted, and a temperature correction scheme based on a Nusselt–Reynolds number dependence was used.

The probe was roughly aligned with the mean flow vector (interpolated from the seven-hole measurements) at each data point location, and small samples of measurements were taken (about 500 samples). These samples were processed on-line, and the probe was realigned to the newly measured mean flow velocity vector. This process was repeated until the probe was aligned to within 1 deg of the mean velocity vector. When the probe was determined to be aligned with the local mean flow, a full sample buffer of data was taken. At each data point, a total of 10,000 samples were obtained at a sampling frequency of 500 Hz.

Crossflow planes measured by the triple-wire probe were obtained at the following streamwise stations: $x/c = \pm 0.394, \pm 0.296, \pm 0.197, \pm 0.114, \pm 0.005, 0.005, 0.125, 0.246, 0.452$, and 0.678. The stretched $20 \times 20$ grid focused mainly on the region in the vicinity of the vortex and hence was much smaller than planes measured with the seven-hole probe. The $8 \times 8$ in. ($0.2 \times 0.2$ m) square planes were centered at the nominal core center.

The uncertainties of the hot-wire rms velocity and stress measurements were estimated to be 2.5% for $\hat{u}$ and $\hat{v}$, 3.2% for $\hat{w}$, and the shear stresses $\overline{u'v'}$, $\overline{u'w'}$, and $\overline{v'w'}$ within 15, 15, and 30%, respectively (where $u'v'$, $u'w'$, and $v'w'$ are components of Reynolds shear stress). Velocity gradient corrections were applied to the hot-wire measurements as described in Ref. 18.

As in all probe-based measurements, velocity gradients can lead to additional error. The effect of flow gradients on the mean axial-velocity magnitude, measured by the seven-hole probe, in the core is of particular interest. An estimate of the additional error because of flow gradients in the core can be made by considering a vortex with a core radius of 1.5 in. (0.04 m, a characteristic size in this case) and a maximum tangential velocity of $1.0U_\infty$. A simple calculation shows that the worst-case tangential velocity variation across the face of the probe (0.1-in. or 2.54-mm diam) would be $0.066U_\infty$. This leads to an estimation of a possible flow-angle measurement error of 2.2 deg. In the core, the streamwise pressure gradient variation effect on the measurement uncertainty is negligible. The maximum error in core-axial-velocity magnitude measurement is 0.1% (as a result of the 2.2-deg angle measurement error) above the 1.1% estimated velocity magnitude uncertainty. Because of this low measurement uncertainty, no corrections have been applied to the pressure-probe data.

The possibility of meandering of the vortex was investigated by using a pair of single-wire probes placed on opposite sides of the vortex core ($0.07c$ from the center at $x/c = 0.678$) and evaluating measurements between the two. The wires were aligned so that they were primarily sensitive to velocity fluctuations in the $y$ and $z$ directions. The correlation of fluctuating velocities $\overline{u_1' u_2'}$ was obtained by taking a total of 50,000 samples at a sampling frequency of 2000 Hz and a filter frequency setting of 50 Hz.

Data were acquired with a 32-bit DEC $\mu$VAX II computer and a 15-bit Tustin X-2100 A/D. Measurement error as a result of A/D resolution was negligible compared with instrumentation error.

## Results and Discussion

Figure 3 displays normalized crossflow velocity magnitude at various crossflow planes ($x/c = \pm 0.591, \pm 0.394, \pm 0.197, \pm 0.005, 0.125, 0.246, 0.452$, and 0.678) measured by the seven-hole pressure probe. The crossflow planes are displayed in conjunction with the wing and the root wall. The farthest upstream plane, at $x/c = \pm 0.59$, shows high crossflow velocity circumventing the tip, but no tip vortex is evident at this location. As $x$ increases, the region of high-crossflow velocity increases (in both area and magnitude) as the tip vortex gains strength from the feeding sheet of boundary layer vorticity. The first indication of a tip vortex is seen in the second data plane at $x/c = \pm 0.394$. Small patches of low-crossflow-velocity fluid can be seen between the feeding sheet and the main vortex, corresponding to the approximate location where the oil flow showed evidence of a small secondary vortex. These patches of low-crossflow velocity are not readily observable in data planes taken in the wake ($x/c \geq 0.0$). In each plane, crossflow velocity approaches zero in the core of the vortex. Maximum crossflow velocity (on the order of the freestream velocity) is found on the viscous/inviscid boundary of the vortex. The core radius, $r_1$, was estimated by determining the distance from the point of minimum crossflow velocity in the core to the point of maximum crossflow velocity. Admittedly, for a tip vortex that is still developing, this definition is a bit arbitrary, but it is deemed adequate as a general descriptor. The radius of the viscous core of the main tip vortex at $x/c = \pm 0.197$ was found to be about 1.0 in. (25.4 mm).

Also shown in Fig. 3 are the normalized axial velocity contours at the same locations and perspective as that of the crossflow velocity. Again, the axial development of the tip vortex is apparent from the progression of data planes. The axial velocity in the core of the vortex increases with $x$, and a maximum axial velocity of $1.77U_\infty$ was obtained at $x/c = \pm 0.005$ (just upstream of the trailing edge). Chigier and Corsiglia[9] noted a maximum axial velocity in the core near the trailing edge of about $1.4U_\infty$ (NACA 0015, at $\alpha = 12.0$ deg, $Re_c = 953 \times 10^3$). Immediately downstream of the trailing edge, they observed an axial core velocity reduction to $1.1U_\infty$. In this

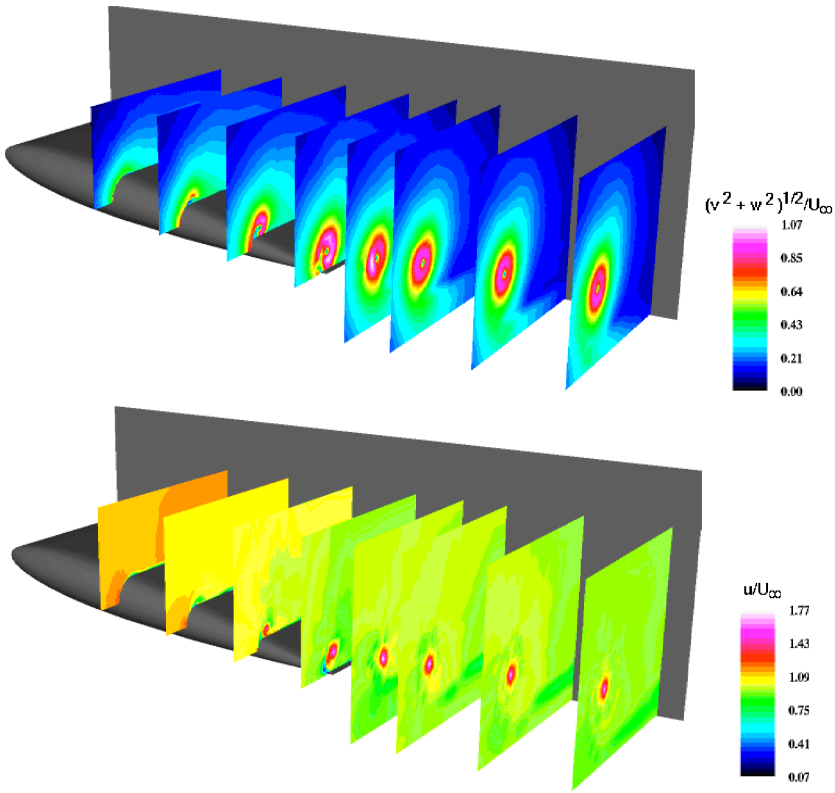


**Fig. 3 Normalized crossflow and axial velocity contours.**



study, the axial velocity maximum decreases very slowly in the wake to a value of $1.69U_\infty$ at $x/c = 0.678$, a marked difference from the results of Chigier and Corsiglia.

Various flow quantities as a function of $x/c$ along the center of the vortex (location of minimum core crossflow velocity) are presented in Fig. 4. Axial velocity, static pressure and total pressure coefficient, and position of the core centerline are plotted. At $x/c = -0.394$, where the tip vortex is first evident, the core axial velocity is $0.82U_\infty$ (a slight velocity deficit), and the static pressure is below freestream static. Until the trailing edge plane is reached (data at $x/c = -0.005$ and 0.005 straddle the trailing edge), the general trend of Fig. 4 shows that the total and static pressure fall and the axial velocity increases with increasing $x/c$. The rate at which the static pressure falls is much faster than the rate of total pressure decrease.

The large favorable axial pressure gradient in the core of the vortex is related to development of large axial velocity excess as shown by radial momentum balance. In the wake planes, the core axial velocity decreases slowly and the static pressure levels off. The low absolute level of the total pressure coefficient ($C_{p,\text{tot}}$ is significantly less than 1 and decreasing) implies that the flow in the vortex core has suffered from viscous losses, which is not surprising considering that much of the vortex fluid originates from the detached boundary layers.

The location of the core is plotted in the bottom panel of Fig. 4. Contrary to what has been observed in free air wingtip vortices, the vortex moves up and slightly outboard with respect to the trailing edge and tip. This is an inviscid effect caused by the close proximity of the wind-tunnel walls and should have little or no effect on turbulence measurements.

The nondimensional circulation of the vortex was found by taking a line integral of the velocity vector over a closed path in a crossflow plane. The enclosed area formed by this path included 75% of the span, so that much of the vorticity shed by the viscous wake of the wing is included in this calculation. The value was found to be $\Gamma = 0.33$ [where $\Gamma = \text{circulation}/(U_\infty c)$] at $x/c = 0.005$.

As mentioned in the Introduction, many studies of vortices in the far field have been contaminated by meander. In some cases, undetected meander has lead to erroneous conclusions concerning core turbulence levels. Meander is a real phenomenon that is likely to result from amplification of small disturbances in the vicinity of the

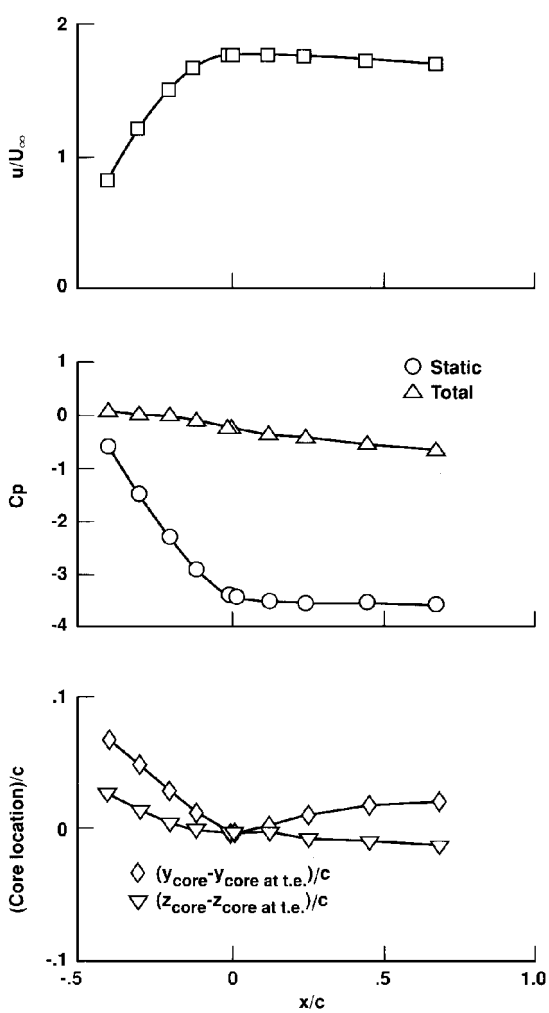


**Fig. 4 Axial progression of various core flow quantities.**

wing. It is thought that meander exists in wind tunnel studies and not in the extremely low freestream-turbulence environment found in flight. Because our near-field measurements indicate high core turbulence levels, it is essential that the question of vortex meander be fully documented so that conclusions drawn about the developing turbulent vortex core be based on real vorticity-bearing turbulence measurements and not simply results of a high-gradient flowfield oscillating through a probe volume.

Previous researchers[14] have found the tip vortex to meander periodically in a spanwise direction with $fc/U_\infty$ on the order of 0.01. Measurements of the velocity correlation $\overline{u_1' u_2'}$ between the two single wires, positioned on opposite sides of the vortex core, were compared with the correlation computed from an analytical model. The measured value of $\overline{u_1' u_2'}$ was $-2.8 \times 10^{-7}$. Mean velocity profiles, measured by seven-hole probe, were used to define the steady functions $u(z)$, $v(z)$, and $w(z)$. These steady functions were used in an analytical model that assumed a sinusoidal meander of the vortex in the lateral direction. The model was then used to assess the effects of meander. The $z$ location, which the modeled single wire saw, was governed by the following equation:

$$z = z_0 + a \sin \omega t \tag{1}$$

where $z_0$ is the actual location of the single-wire probe, $a$ is the amplitude of the sinusoidal meander, and $\omega$ is the frequency.

Assuming an oscillation with a period of 0.4 s ($fc/U_\infty = 0.01$), a meander amplitude of 0.005 in. (0.13 mm, i.e. about $0.00010c$) gave a correlation equal to the experimentally measured correlation. A rough estimate of the effect of meander was then made by assuming a periodic motion in the lateral direction with an amplitude of 0.005 in. (0.13 mm). Given that the velocity gradient in the core of the vortex is approximately $1.0U_\infty$/in., this level of meander could cause an apparent additional rms velocity of 0.5% freestream. By similar analysis, the influence on apparent additional normalized Reynolds shear stress levels could reach levels on the order of 0.000025. These low levels were considered to be negligible. This may not be particularly surprising given that $x/c$ is so small ($<0.678$) and $\alpha$ is relatively large (10 deg).

Cross-stream planes ($y-z$) of turbulence measured by the triple-wire probe are shown in Fig. 5. Data planes are presented at the same streamwise stations as the mean flow data but the physical width and height of these data planes are smaller (width is $0.167c$).

The highest levels of $\hat{u}$, $\hat{v}$, and $\hat{w}$ rms velocity normalized by the freestream velocity (Fig. 5) were measured to be 0.224, 0.228, and 0.246, respectively. The character of the turbulence structure was markedly different in planes measured over the wing and planes measured in the wake. In planes measured over the suction side of the wing, peak levels of turbulence were found where the shear layer departed from the wingtip surface. The levels of rms velocity decrease as this highly turbulent fluid is wrapped into the forming tip vortex. In the vortex, peak levels of turbulence were measured near the location of maximum tangential velocity. This behavior continued at $x/c = 0.005$ and 0.125. In the wake planes farther downstream, however, the peak levels of rms velocity were measured in the center of the vortex. The peak $\hat{u}$, $\hat{v}$, and $\hat{w}$ rms velocity decreased to a level of 0.100, 0.146, and 0.117, respectively, at the final $x/c = 0.678$ station. The stabilizing effects of the trend toward solid body rotation of the vortex seem to dissipate the turbulence at a rapid rate. However, the peak levels measured at $x/c = 0.678$ indicate that, at less than one chord downstream of the trailing edge, the vortex core is still a highly turbulent region. Modelers who ignore this fact will surely predict the rollup incorrectly.

Contours of $\hat{u}$ shown in Fig. 5 are roughly circular, which might be expected for a vortical flow. However, contours of $\hat{v}$ and $\hat{w}$ are not circular. Instead, contours of $\hat{v}$ are roughly elliptical, with the major axes running in the $y$ direction, and contours of $\hat{w}$ are roughly elliptical, with major axes running in the $z$ direction. In cylindrical coordinates, this would represent levels of the rms radial velocity $\hat{v}_r$ (where $\hat{v}_r$, $\hat{v}_\theta$, and $\hat{v}_x$ are the rms velocity components in the $r$, $\theta$, $x$ cylindrical coordinate system) greater than levels of the rms tangential velocity, with $\hat{v}_\theta$ indicating anisotropy. This behavior can explain various other interesting features of the turbulence in the tip vortex flow, including the orientation of the $\overline{v'w'}$ component of the Reynolds stress. The kinematics of how this occurs is detailed later.

High levels of all three Reynolds shear stresses were measured in the vortex, whereas in a vortex with negligible gradients of axial velocity, the only component of shear stress that would exist would be the $\overline{v'w'}$ component. Perspective views of contours of $\overline{u'v'}$, $\overline{u'w'}$, and $\overline{v'w'}$ are plotted in Fig. 5. Overall peak absolute levels of $\overline{u'v'}$, $\overline{u'w'}$, and $\overline{v'w'}$ normalized by the square of the freestream velocity were found to be 0.0125, 0.0234, and 0.0139 at $x/c = -0.197$, $-0.010$, and 0.005, respectively. These peak levels decayed with $x/c$ thereafter, with the farthest downstream plane ($x/c = 0.678$) showing peak levels of 0.0029, 0.0004, and 0.0024 for $\overline{u'v'}$, $\overline{u'w'}$, and $\overline{v'w'}$, respectively.

Qualitatively, contours of the $\overline{v'w'}$ stress in the wake planes ($x/c > 0.0$) had a four-leaf clover pattern with alternately changing sign of stress in each leaf. Each leaf was roughly aligned at $\pm 45$ deg off the $y$ and $z$ axes, with positive levels of stress found in the first and third quadrants ($+/+$ and $-/-$ values of $z$ and $y$, respectively) and negative levels of stress found in the second and fourth quadrants. In addition, in each leaf there seemed to be two radii at where peak levels of stress occurred. At $x/c = 0.452$, these two peaks occurred roughly at $r/r_1 = 0.33$ and 1.8. The four-leaf clover pattern and the two-lobe pattern of the $\overline{u'v'}$ and $\overline{u'w'}$ stresses (described later) is expected for a Cartesian coordinate system, and this can be explained by the following kinematic relations (given that $x = x$, $y = r \cos\theta$, and $z = r \sin\theta$ and $\overline{v_r' v_r'}$ and $\overline{v_\theta' v_\theta'}$ are components of Reynolds shear stress in the cylindrical coordinate system):

$$\overline{u'v'} = -\overline{v_r' v_\theta'} \sin\theta + \overline{v_x' v_r'} \cos\theta \tag{2a}$$

$$\overline{u'w'} = \overline{v_r' v_\theta'} \cos\theta + \overline{v_x' v_r'} \sin\theta \tag{2b}$$

$$\overline{v'w'} = (\overline{v_r'^2} - \overline{v_\theta'^2}) \cos\theta \sin\theta + \overline{v_r' v_\theta'}(\cos^2\theta - \sin^2\theta) \tag{2c}$$

The signs of $\overline{u'v'}$, $\overline{u'w'}$, and $\overline{v'w'}$ in the alternating lobes are entirely dependent on orientation of the Cartesian coordinate system. Therefore, the orientation of the coordinate system in this study should be kept in mind during discussions about the signs of shear stress quantities.

The orientation of the alternately positive and negative regions does have physical implications, however, and closer inspection of Eq. (2c) shows how a $\pm 45$-deg orientation of the $\overline{v'w'}$ stress implies that the $\overline{v_r'^2} > \overline{v_\theta'^2}$ and that $\overline{v_r'^2}$, $\overline{v_\theta'^2} \gg \overline{v_r' v_\theta'}$ (where $\overline{v_r'^2}$ and $\overline{v_\theta'^2}$ are components of the Reynolds normal stress in the cylindrical coordinate system). In confirmation of these kinematics, the measurement of the normal stress contours for $\hat{v}$ and $\hat{w}$ were found to be elliptical. For an explanation of why $\overline{v_r'^2} > \overline{v_\theta'^2}$, see Ref. 18.

Figure 6 displays contours of the Reynolds shear stresses and the negative of their corresponding mean strain rates at $x/c = 0.452$, e.g., $\partial v/\partial z + \partial w/\partial y$ for the $\overline{v'w'}$ stress. The shapes of these contours would be oriented in the same direction if the flow were isotropic. Clearly, this is not the case. Noticeably, for each stress, the strain rate is aligned almost exactly opposite what would be expected for an isotropic eddy viscosity. An explanation for this is given by Chow et al.[18]

The structure of the contours of $\overline{v'w'}$ was not as clear in the planes measured over the wing ($x/c < 0.0$). Although the beginnings of the four-leaf clover pattern can be seen, the influence of the stress created by the shear layers heavily distorts it.

Contours of $\overline{u'v'}$ in the wake planes had two lobes of opposite-sign stress, with the positive lobe rotated about 30 deg off the $z$ axis. The peak levels of stress at a $x/c = 0.452$ occurred at a radius of about $r/r_1 = 0.33$, which corresponds with the first peak measured in the $\overline{v'w'}$ stress.

Contours of $\overline{u'w'}$ in the wake planes had two lobes of opposite sign stress, with the positive lobe rotated about 20 deg off the negative $y$ axis. Closer analysis of the kinematic Eqs. (2a) and (2b) show that $\overline{v_x' v_r'}$ and $\overline{v_x' v_\theta'}$ are both positive and roughly of the same magnitude. Again, peak levels of stress occurred at a radius of about $r/r_1 = 0.33$ for $x/c = 0.452$. Peak levels of all shear stresses at $x/c = 0.125$, however, were measured at a radius of roughly $r/r_1 = 0.67$, a clearly marked difference in behavior from the peaks measured farther downstream.

Figure 7 shows $v_\theta$ and $\partial v_x/\partial r$ vs $y$ distance from the vortex centerline at $x/c = 0.125$ and 0.452, respectively; $v_\theta$ is plotted

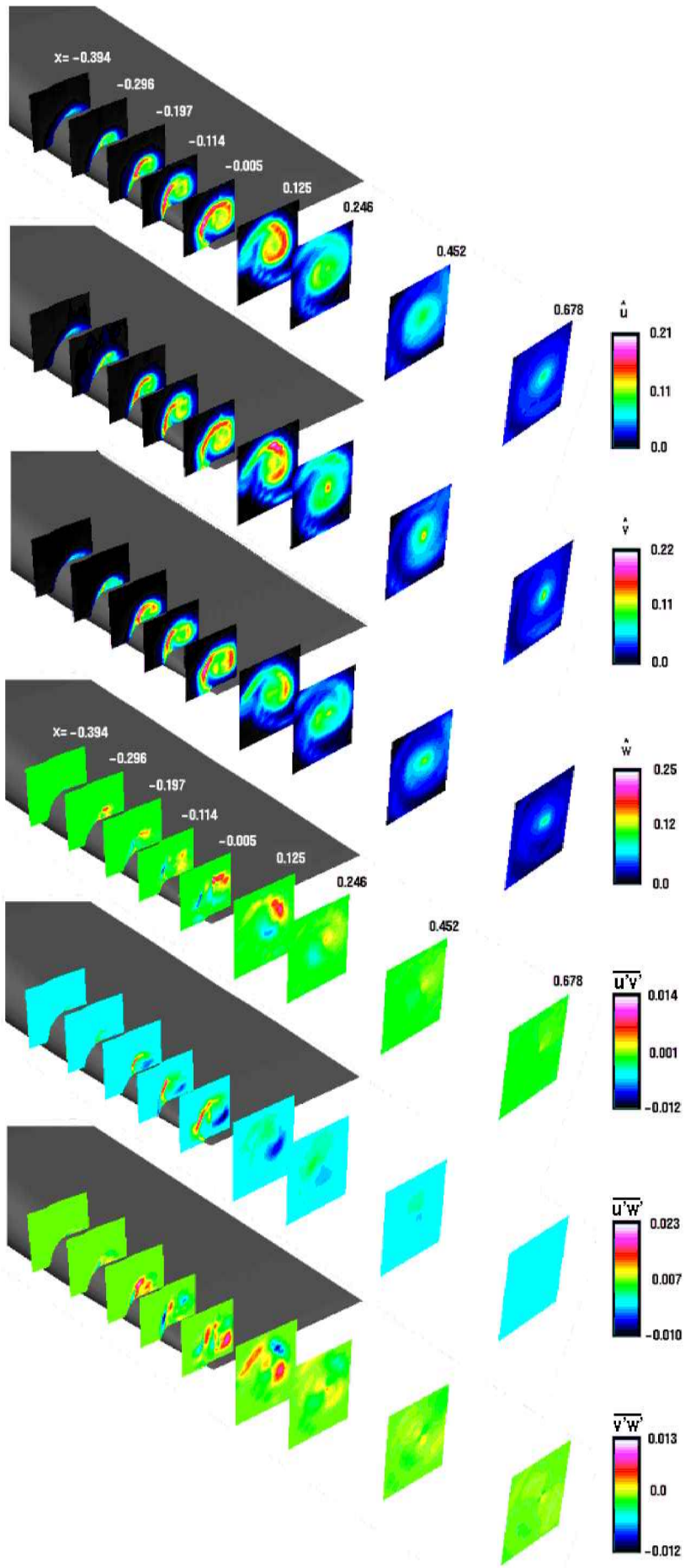


**Fig. 5 Perspective view of the rms velocity and Reynolds shear stress components.**

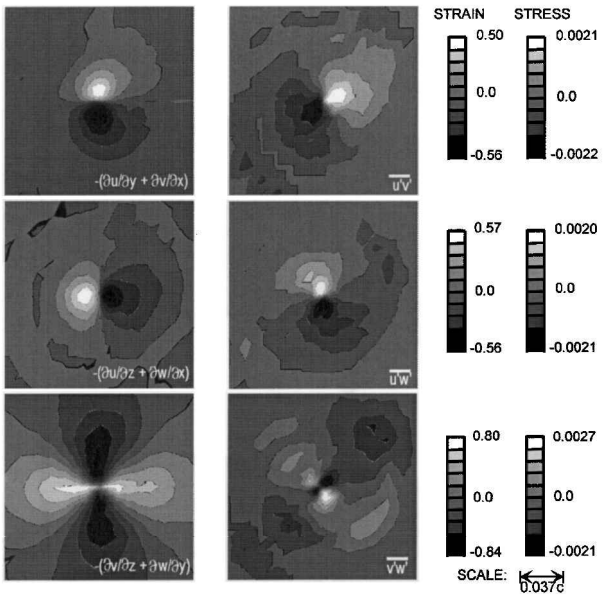


**Fig. 6 Contours of mean strain rate and respective Reynolds stress.**

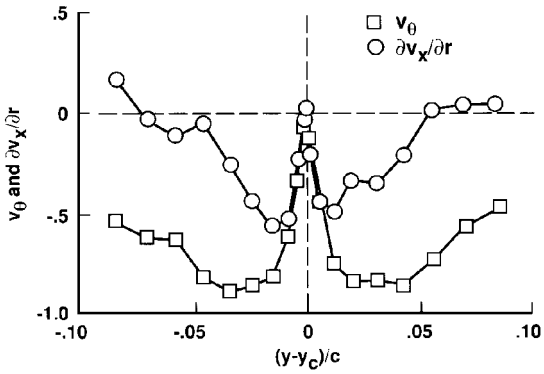


**Fig. 7 Plot of $v_\theta$ and $\partial v_x/\partial r$ vs $y$ distance at $x/c = 0.125$.**

only to aid in estimating $r_1$. The peak levels of $\partial v_x/\partial r$ occur at $r/r_1 \approx 0.40$. The radial gradient of the mean axial velocity in the vortex core is the main cause of turbulent production in the near wake. Chow et al.[18] give a more detailed analysis of this (and of other aspects of the turbulent structure) through a comparison of the production terms in the turbulence transport equations.

## Conclusions

The complete mean flowfield and the complete Reynolds stress tensor have been measured in the near field of a turbulent wing tip vortex. The knowledge gained should be of great use to those interested in accurate modeling of vortex-dominated flows as well as to aircraft designers. The major findings of this study are as follows.

1) Development of the crossflow velocities with chordwise distance induced a favorable axial pressure gradient in the core, resulting in acceleration of the core centerline fluid to 1.77 times the freestream velocity. The factors contributing to this high level of core axial velocity, relative to what has been measured in the past, include the high incidence of the wind-tunnel model, the relatively high Reynolds number of the study, and the smoothness of the tip geometry (squared-off tips would behave differently). In addition, few studies have focused so intensely on the near field, so it is likely that this aspect of the flowfield has been overlooked.

2) Turbulence levels in and around the vortex core were initially very large. This was primarily because of turbulence originating in the wingtip tip-boundary layers being wrapped into the rollup of the vortex.

3) Peak turbulence levels in data planes measured over the wing were found to be located near the edge of the viscous core of the vortex. A short distance downstream, however, the location of the peak levels shifted from the edge of the viscous core, $r/r_1 \approx 1$, to a location at a much smaller radius, $r/r_1 \approx 0.33$, which was roughly where $\partial v_x/\partial r$ was maximum. In addition, the peak levels decreased downstream of the trailing edge.

4) Although additional turbulence was generated by the mean axial velocity gradients downstream of the trailing edge, it appears that the relaminarizing influence of the solid body rotation has a much larger effect, resulting in the extraordinary decay rate of the overall turbulence in the vortex. This is consistent with the results of Devenport et al.,[15] who found that, in the range of $x/c = 5.0$–$30.0$, the core region was laminar.

5) Kinematically, the anisotropy of the normal stresses and the low levels of $\overline{v_t v_\theta}$ stress result in contours of $\overline{v_t w_t}$ stress shifted 45 deg from the corresponding mean strain rate. The fact that the stress lags the strain rate bodes ill for isotropic eddy-viscosity methods.

The data acquired during this study are available (with certain restrictions) and can be obtained by contacting the authors.

## Acknowledgments

The authors wish to thank Jennifer Dacles-Mariani and Rabindra Mehta of NASA Ames Research Center and to acknowledge the late Otto Zeman for helpful suggestions and discussions.

## References

[1]Dacles-Mariani, J., Zilliac, G. G., Chow, J., and Bradshaw, P., "Numerical/Experimental Study of a Wingtip Vortex in the Near Field," *AIAA Journal*, Vol. 33, No. 9, 1995, pp. 1561–1568.

[2]Hoffman, E. R., and Joubert, J., "Turbulent Line Vortices," *Journal of Fluid Mechanics*, Vol. 16, Pt. 3, 1963, pp. 395–411.

[3]Batchelor, G. K., "Axial Flow in Trailing Line Vortices," *Journal of Fluid Mechanics*, Vol. 20, Pt. 4, 1964, pp. 645–658.

[4]Moore, D. W., and Saffman, P. G., "Axial Flow in Laminar Trailing Vortices," *Proceedings of the Royal Society of London*, Vol. 333, 1973, pp. 491–508.

[5]Squire, H. B., "The Growth of a Vortex in Turbulent Flow," *Aeronautical Quarterly*, Vol. 16, Pt. 3, 1965, pp. 302–306.

[6]Spivey, R. F., "Blade Tip Aerodynamics, Profile and Planform Effects," *Twenty-Fourth Annual National Forum of the American Helicopter Society*, American Helicopter Society, Washington, DC, 1968.

[7]Carlin, G., Dadone, L., and Spencer, R., "Results of an Experimental Investigation of Blade Tip Vortex Modification Devices," NASA CR-181853, June 1989.

[8]Spivey, W. A., and Morehouse, G. G., "New Insights Into the Design of Swept-Tip Rotor Blades," *Twenty-Sixth Annual National Forum of the American Helicopter Society*, American Helicopter Society, Washington, DC, 1970.

[9]Chigier, N. A., and Corsiglia, V. R., "Tip Vortices—Velocity Distributions," NASA TM X-62,087, Sept. 1971.

[10]Green, S. I., "Correlating Single Phase Flow Measurements with Observations of Trailing Vortex Cavitation," *Journal of Fluids Engineering*, Vol. 113, No. 1, 1991, pp. 125–129.

[11]Mehta, R. D., and Cantwell, E. R., "Mean Flow and Turbulent Measurements in a Half-Delta Wing Vortex," *Fluid Dynamics Research*, Vol. 4, No. 2, 1988, pp. 123–137.

[12]Bandyopadhyay, P. R., Stead, D. J., and Ash, R. L., "The Organized Nature of a Turbulent Trailing Vortex," *AIAA Journal*, Vol. 29, No. 10, 1990, pp. 1627–1633.

[13]Westphal, R. V., and Mehta, R. D., "Interaction of an Oscillating Vortex with a Turbulent Boundary Layer," *Experiments in Fluids*, Vol. 7, No. 6, 1989, pp. 405–411.

[14]McAlister, K. W., and Takahashi, R. K., "NACA 0015 Wing Pressure and Trailing Vortex Measurements," NASA TP-3151, Nov. 1991.

[15]Devenport, W. J., Rife, M. C., Liapis, S. I., and Follin, G. J., "Turbulent Structure and Scaling in Trailing Vortices," AIAA 33rd Aerospace Sciences Meeting and Exhibit, Reno, NV, Jan. 1995.

[16]Zilliac, G., "Calibration of Seven-Hole Pressure Probes for Use in Fluid Flows with Large Angularity," NASA TM 102200, Dec. 1989.

[17]LeBoeuf, R. L., "Application of the Proper Orthogonal Decomposition Techniques to an Annular Cascade Flowfield," Ph.D. Dissertation, Dept. of Mechanical and Aerospace Engineering, State Univ. of New York, Buffalo, NY, June 1991.

[18]Chow, J. S., Zilliac, G. G., and Bradshaw, P., "Turbulence Measurements in the Near-Field of a Wingtip Vortex," NASA TM 110418, Feb. 1997.

R. W. Wlezien
*Associate Editor*

**Color reproduction courtesy of NASA Ames Research Center**